

# Electronic state calculations of ultrasmall Si quantum boxes: Quasialloying and surface effects on the electronic and optical properties

Masahiko Nishida

*Academic Foundations Program, Kanazawa Institute of Technology, Nonoichi-machi, Ishikawa 921-8501, Japan*

(Received 2 February 2010; revised manuscript received 22 April 2010; published 4 June 2010)

Energy gaps and oscillator strengths of ultrasmall Si  $5_{[1\bar{1}0]} \times 5_{[110]} \times N_{z[001]}$ ,  $N_{x[1\bar{1}0]} \times 5_{[110]} \times 5_{[001]}$ , and  $5_{[100]} \times 5_{[010]} \times N_{z[001]}$  quantum boxes (QBs) passivated by hydrogen are calculated and compared with those of Si quantum spheres. Although the  $5_{[1\bar{1}0]} \times 5_{[110]} \times N_{z[001]}$  QB suggests an effect of weaker (two-dimensional) quantum confinement than the  $N_{x[1\bar{1}0]} \times 5_{[110]} \times 5_{[001]}$  QB, the former exhibits a larger energy gap than the latter. This is not explained by the quantum-confinement model alone but by an effect of quasialloying between H and Si on the highest occupied molecular orbital level, which is sensitive to the shape of the ultrasmall Si QBs and can contribute to the widening of the energy gap. It is found that the oscillator strength calculated for the  $N_{x[1\bar{1}0]} \times 5_{[110]} \times 5_{[001]}$  and the  $5_{[1\bar{1}0]} \times 5_{[110]} \times N_{z[001]}$  QBs is well controlled by (two-dimensional) quantum confinement whereas that for the  $5_{[100]} \times 5_{[010]} \times N_{z[001]}$  QB is not. The latter is explained by the occurrence of a H-related surface state at the lowest unoccupied molecular orbital level, which is also sensitive to the shape of the QBs.

DOI: 10.1103/PhysRevB.81.235306

PACS number(s): 73.21.La, 73.22.Dj, 78.67.Bf

## I. INTRODUCTION

A highly advanced technology in today's microelectronics is based on Si. Unfortunately, Si is an indirect band-gap (1.13 eV) semiconductor and therefore cannot be used directly in optical devices. If Si-based light-emitting devices are realized, it is highly expected that optoelectronics monolithically integrated by using conventional Si processing steps established on Si substrates is developed. Thus, the light-emitting components made up of Si are essentially needed. For the purpose of engineering the Si band gap, so far, a variety of approaches have been taken based on reduced dimensionality inducing quantum-confinement effects, including porous Si,<sup>1</sup> nanocrystalline Si,<sup>2</sup> Si nanowires,<sup>3</sup> Si/Ge alloy or superlattices,<sup>4</sup> and Si/SiO<sub>2</sub> superlattices.<sup>5</sup> Recently, a different approach has also been proposed based on superlattices composed of two ultrathin Si films with different thicknesses.<sup>6</sup>

In the past, Si nanocrystals in porous Si and in a matrix of oxides have been of great interest.<sup>1,2</sup> As is well known, Si nanocrystals passivated with hydrogen are contained in as-prepared porous Si, which exhibit enhanced photoluminescence (PL) spectra in the visible.<sup>1</sup> The observation of blue-shifts in the peak energy of PL has been explained by the widely used quantum-confinement model. However, various surface-sensitive emission processes observed in as-prepared porous Si cannot be explained by the quantum-confinement model alone.<sup>1</sup> The true mechanism remains unsolved. In theoretical aspects, so far, studies on Si nanocrystals have focused on quantum spheres, though porous Si should contain nanocrystals with various shapes. Theoretical works on the dependence of the electronic and optical properties of Si nanocrystals on the shape have been reported previously.<sup>7,8</sup> However, all calculated results reported there have been discussed by using the quantum-confinement model alone.

In this paper, the electronic structure of three types of ultrasmall Si quantum boxes (QBs) passivated with hydrogen is calculated and compared with that of Si quantum spheres.

The present theoretical study focuses on a correlation of the highest occupied molecular orbital (HOMO) and lowest unoccupied molecular orbital (LUMO) levels with hydrogen. It is shown that hydrogen can be more closely involved in the electronic and optical properties of the QBs than expected, and that calculated properties cannot be explained solely by the quantum-confinement model. More specifically, it is found that, in addition to a quantum-confinement effect, an effect of quasialloying between H and Si on the HOMO level, which is sensitive to the shape of the ultrasmall Si QBs, can contribute significantly to the widening of the energy gap, and that the oscillator strength is not always controlled by quantum confinement but is sensitive to whether the LUMO level is, depending on the shape of the QBs, bulklike or surfacelike in nature.

## II. MODEL AND CALCULATIONS

There are two types of geometry for Si quantum spheres studied: one with a central atom and the other with a tetrahedral interstitial at the center. Specifically, Si quantum spheres studied are constructed by starting with a central Si atom or a tetrahedral interstitial at the center, and sequentially adding its nearest-neighbor shells of Si atoms up to the 13th one. Dangling bonds occurring on the surface are passivated with hydrogen atoms along the tetrahedral bond directions. For example, the Si<sub>29</sub>(H<sub>36</sub>) and Si<sub>191</sub>(H<sub>148</sub>) quantum spheres have a configuration with a central Si atom while the Si<sub>30</sub>(H<sub>40</sub>) and Si<sub>196</sub>(H<sub>144</sub>) quantum spheres have a configuration with a tetrahedral interstitial at the center. The Si<sub>29</sub>(H<sub>36</sub>) and Si<sub>30</sub>(H<sub>40</sub>) spheres are of ~1 nm in diameter and the Si<sub>191</sub>(H<sub>148</sub>) and Si<sub>196</sub>(H<sub>144</sub>) spheres are of ~2 nm in diameter.

On the other hand, we study three types of Si QBs. One is referred to as a  $5_{[100]} \times 5_{[010]} \times N_{z[001]}$  QB with {100} planes on the surface. Here,  $5_{[100]}$ ,  $5_{[010]}$ , and  $N_{z[001]}$  ( $N_z = 5, 7, 9, \dots$ ) stand for the number of Si monolayers along the [100], [010], and [001] directions, respectively. Other two

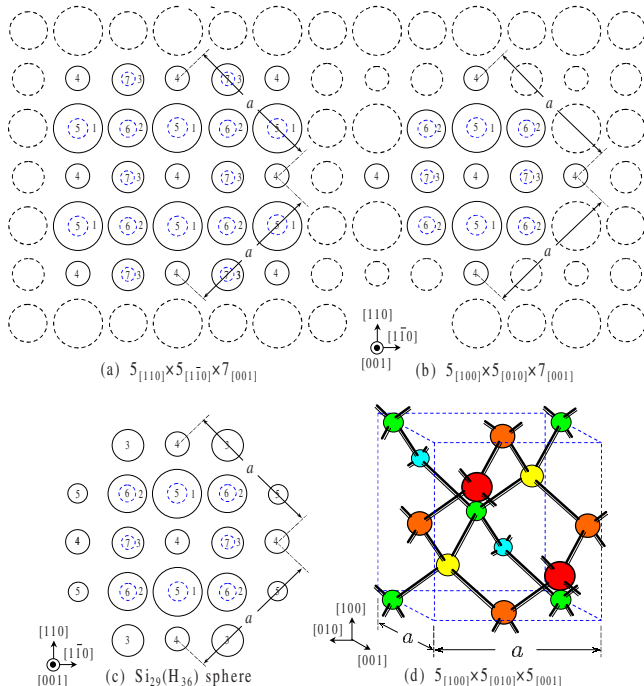


FIG. 1. (Color online) Schematic plan [along the (001) plane] of the Si-atom configuration for the (a)  $5_{[1\bar{1}0]} \times 5_{[110]} \times 7_{[001]}$  quantum box (QB), each side of which is  $\sqrt{2}a$  ( $a$  is the lattice constant) along the (001) surface, (b)  $5_{[100]} \times 5_{[010]} \times 7_{[001]}$  QB, each side of which is  $a$ , and (c)  $\text{Si}_{29}(\text{H}_{36})$  sphere, as viewed along the  $[001]$  direction, and (d) three-dimensional illustration of the  $5_{[100]} \times 5_{[010]} \times 5_{[001]}$  QB. Silicon atoms contained in a QB are denoted by solid circles. The dotted circles denote the Si atoms at their bulk positions outside the QB under study. The size of a circle indicates the proximity of that atom to the (001) surface. A number given to each Si atom denotes the atomic layer in which it lies along the  $[00\bar{1}]$  direction. The Si atoms denoted by the smaller dotted circles labeled 5, 6, and 7 lies exactly below the ones labeled 1, 2, and 3, respectively. Hydrogen atoms saturating dangling bonds are not shown for simplicity.

are referred to as  $5_{[1\bar{1}0]} \times 5_{[110]} \times N_{z[001]}$  and  $N_{x[1\bar{1}0]} \times 5_{[110]} \times 5_{[001]}$  QBs with  $(1\bar{1}0)$ ,  $(110)$ , and  $(001)$  planes on the surface, where  $N_{x[1\bar{1}0]}$  ( $N_x=5, 7, 9, \dots$ ) and  $5_{[110]}$  denote the number of Si monolayers along the  $[1\bar{1}0]$  and  $[110]$  directions, respectively.

Figure 1 shows a top view of the atomic configuration for (a) the  $5_{[1\bar{1}0]} \times 5_{[110]} \times 7_{[001]}$  QB, each side of which is  $\sqrt{2}a$  ( $a$  is the lattice constant) along the (001) plane and (b) the  $5_{[100]} \times 5_{[010]} \times 7_{[001]}$  QB (each side is  $a$ ), as viewed along the  $[001]$  direction. The atomic configuration for the  $\text{Si}_{29}(\text{H}_{36})$  sphere is shown in Fig. 1(c) for the sake of comparison. Figure 1(d) schematically illustrates a three-dimensional structure of the  $5_{[100]} \times 5_{[010]} \times 5_{[001]}$  QB for clarity. Hydrogen atoms passivating the resulting dangling bonds are not shown in Fig. 1 for simplicity. The  $5_{[100]} \times 5_{[010]} \times N_{z[001]}$  QB ( $N_z=5, 7, 9, \dots$ ), for example, is constructed by sequentially adding Si atoms along the  $[00\bar{1}]$  direction as follows. One starts with the  $5_{[100]} \times 5_{[010]} \times 5_{[001]}$  QB shown in Fig. 1(d), and then puts four and two Si atoms on the sixth and seventh monolayer exactly below the

Si atoms labeled 2 and 3 in Fig. 1(b), respectively, thereby creating a  $5_{[100]} \times 5_{[010]} \times 7_{[001]}$  QB. Next, one can produce a  $5_{[100]} \times 5_{[010]} \times 9_{[001]}$  QB by adding five and two Si atoms on the eighth and ninth monolayer exactly below the Si atoms labeled 4 and 5 in Fig. 1(b), respectively.

Electronic state calculations are performed using the extended Hückel-type nonorthogonal tight-binding (EHNTB) method.<sup>9</sup> In the EHNTB scheme, all distant-neighbor nonorthogonal overlap and energy integrals between atomic orbitals (simulated by Slater-type atomic orbitals) centered on each atom in a nanocrystal are explicitly calculated up to the sixth-nearest neighbors. The EHNTB parameters associated with Si were so adjusted that the calculated band structure agrees with other sophisticated calculations and experiment to the fullest possible extent. In particular, special care was given to the quantitatively precise reproduction of the conduction and valence bands across the Brillouin zone by the EHNTB method, thereby enabling one to study the optical properties of Si nanostructures. The interaction parameters between Si and H and between H and H were determined by fitting calculated H-related (bonding and antibonding) surface states to experimental data on the H-covered Si(111) surface, which was most intensively studied. The band structure of bulk Si and the EHNTB parameters thus determined are given in Ref. 9. For studying the energy gap between the HOMO and LUMO levels in Si nanocrystals, it is noted that the EHNTB scheme does not give any energy-gap problem such as that in density functional theory (DFT) because the parameters are adjusted in the EHNTB scheme while no parameters are adjusted within the DFT framework.

In the EHNTB scheme, usually, relaxation is not explicitly given to atomic coordinates. Instead, we can use a reasonable relaxed structure determined by first-principles calculations in literature. Specifically, a first-principles calculation has determined the relaxed Si-Si and Si-H lengths for the ultras-small  $\text{Si}_{29}\text{H}_{36}$  quantum sphere, including every effect due to relaxation.<sup>10</sup> The values determined for the relaxed Si-Si and Si-H lengths are 2.352 Å and 1.500 Å, respectively. These values are used for the present EHNTB calculations. It is noted that the values determined for the relaxed bonds are only slightly (0.08% and 1.3%) larger than 2.35 Å and 1.48 Å that are for the Si bulk and a covalent Si-H bond, respectively, even for a Si nanocrystal as small as the  $\text{Si}_{29}(\text{H}_{36})$  sphere. Also, other first-principles calculations for Si nanocrystals passivated with hydrogen have shown that relaxation introduces only several percent change (expansion or contraction) in the Si-Si length even in the excited state.<sup>11,12</sup> Thus, we can say that the introduction of relaxation does not give a significantly large change to the atomic coordinates in Si nanocrystals, as suggested by these first-principles calculations.<sup>10-12</sup>

In Fig. 1, the atomic configurations of the (a)  $5_{[1\bar{1}0]} \times 5_{[110]} \times 7_{[001]}$  QB, (b)  $5_{[100]} \times 5_{[010]} \times 7_{[001]}$  QB, and (c)  $\text{Si}_{29}(\text{H}_{36})$  sphere are illustrated, for the purpose of showing that these three nanocrystals are roughly on a similar size level. While the  $5_{[100]} \times 5_{[010]} \times N_{z[001]}$  QB is smaller by two Si monolayers than the  $\text{Si}_{29}(\text{H}_{36})$  sphere along the  $[100]$  and  $[010]$  directions, the  $5_{[1\bar{1}0]} \times 5_{[110]} \times N_{z[001]}$  QB is the same in size as the  $\text{Si}_{29}(\text{H}_{36})$  sphere along the  $\langle 110 \rangle$  directions. Therefore, it would be reasonable to apply the same bond

lengths as the ones determined for the  $\text{Si}_{29}(\text{H}_{36})$  sphere to the QBs as well as the quantum spheres studied here.

With the aim of analyzing the nature of HOMO and LUMO states, the orbital density of states (ODOS) for orbital  $i$  at energy  $\varepsilon$  is calculated by giving each energy level a Gaussian broadening with a half width ( $\omega$ ) of 0.05 eV,<sup>13</sup>

$$D_i(\varepsilon) = \frac{2}{\sqrt{\pi\omega}} \sum_n C_{in} \sum_j C_{jn} S_{ij}^n \exp\left[-\frac{(\varepsilon - \varepsilon_n)^2}{\omega^2}\right], \quad (1)$$

where  $\varepsilon_n$  is the  $n$ th eigenvalue (MO energy) of the system,  $C_{in}$ 's the MO coefficients, and  $S_{ij}^n$  the overlap integral between the  $i$ th and  $j$ th orbitals in the  $n$ th MO.

The oscillator strength  $f$  for transitions between HOMO and LUMO states is calculated by the following equation:<sup>14</sup>

$$f = \frac{2}{3mE_g} \langle \psi_H | \mathbf{p} | \psi_L \rangle^2, \quad (2)$$

where  $E_g$  is the energy gap between the HOMO and LUMO states,  $m$  the electron mass, and  $\langle \psi_H | \mathbf{p} | \psi_L \rangle$  is the momentum matrix element between the HOMO and LUMO states for unpolarized light, which is, in the EHNTB scheme, calculated directly from a linear combination of momentum matrix elements between atomic orbitals simulated by Slater-type atomic orbitals. When some almost degenerate states occur at the HOMO or LUMO level, we average the oscillator strength over those degenerate states (to within  $kT_{\text{room}} = 26$  meV). The radiative lifetime  $\tau$  is calculated from the oscillator strength  $f$ ,<sup>14</sup>

$$\frac{1}{\tau} = \frac{ke^2 E_g^2 f}{2\pi\epsilon_0 mc^3 \hbar^2}, \quad (3)$$

where  $k$  is the refractive index ( $k=2.6$  for a Si nanocrystallite<sup>15</sup>),  $e$  the electronic charge,  $\epsilon_0$  the electric permittivity of free space, and  $c$  the speed of light.

### III. RESULTS AND DISCUSSION

#### A. Energy gap

The calculated energy gaps are shown in Fig. 2 as a function of the number of Si atoms for three types of QBs under study:  $5_{[1\bar{1}0]} \times 5_{[110]} \times N_{z[001]}$ ,  $N_{x[1\bar{1}0]} \times 5_{[110]} \times 5_{[001]}$ , and  $5_{[100]} \times 5_{[010]} \times N_{z[001]}$  QBs, in comparison with the energy gaps calculated for the quantum spheres. We can see the overall size dependence of the energy gaps, as expected from the quantum-confinement model. It is found that for a smaller number of Si atoms, the energy gap is not sensitive to the shape while for a larger number of Si atoms, the energy gap is determined by two-dimensional quantum confinement perpendicular to the  $[001]$  direction for the  $5_{[1\bar{1}0]} \times 5_{[110]} \times N_{z[001]}$  and  $5_{[100]} \times 5_{[010]} \times N_{z[001]}$  QBs, and to the  $[1\bar{1}0]$  direction for the  $N_{x[1\bar{1}0]} \times 5_{[110]} \times 5_{[001]}$  QB. On the other hand, the energy gap for the quantum spheres is controlled by three-dimensional quantum confinement for all number of Si atoms studied. Therefore, we can say that for the nanocrystals with Si atoms as many as 100 and more, we can expect that the QBs give a larger energy gap than the spheres.

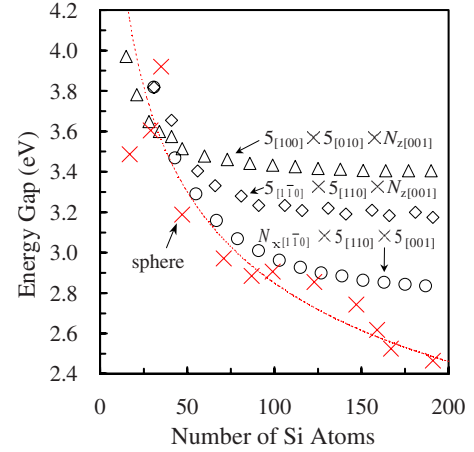


FIG. 2. (Color online) Calculated energy gaps between the HOMO and LUMO levels as a function of the number of Si atoms contained in the QBs and quantum spheres studied. The dashed curve denotes a line determined by the method of least squares for the quantum spheres.

Figure 3 represents the cross sections along the (001) plane for the (a)  $5_{[1\bar{1}0]} \times 5_{[110]} \times N_{z[001]}$  and (b)  $5_{[100]} \times 5_{[010]} \times N_{z[001]}$  QBs, and (c) the cross section along the  $(1\bar{1}0)$  plane for the  $N_{x[1\bar{1}0]} \times 5_{[110]} \times 5_{[001]}$  QB. It is reasonable that the  $5_{[100]} \times 5_{[010]} \times N_{z[001]}$  QB gives the largest energy gap determined by two-dimensional quantum confinement, reflecting the smallest cross section. However, the  $5_{[1\bar{1}0]} \times 5_{[110]} \times N_{z[001]}$  QB exhibits a larger energy gap than the  $N_{x[1\bar{1}0]} \times 5_{[110]} \times 5_{[001]}$  QB. This is strange because the cross section of the  $5_{[1\bar{1}0]} \times 5_{[110]} \times N_{z[001]}$  QB is evidently larger than that of the  $N_{x[1\bar{1}0]} \times 5_{[110]} \times 5_{[001]}$  QB, as shown in Fig. 3, suggesting a weaker effect of two-dimensional quantum confinement in the former QB. Obviously, this needs some physical explanation other than the one based on the quantum-confinement model.

Actually, the variation in the energy gap with the increase in the number of Si atoms contained arises mostly from the downward energy shift of the HOMO level for all Si nanocrystals studied here because the LUMO energies are not very sensitive to the variation in the number of Si atoms

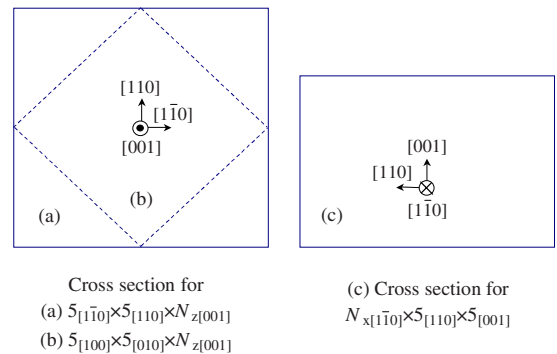


FIG. 3. (Color online) Cross sections along the (001) plane for the (a)  $5_{[1\bar{1}0]} \times 5_{[110]} \times N_{z[001]}$  and (b)  $5_{[100]} \times 5_{[010]} \times N_{z[001]}$  QBs, and (c) cross section along the  $(1\bar{1}0)$  plane for the  $N_{x[1\bar{1}0]} \times 5_{[110]} \times 5_{[001]}$  QB.

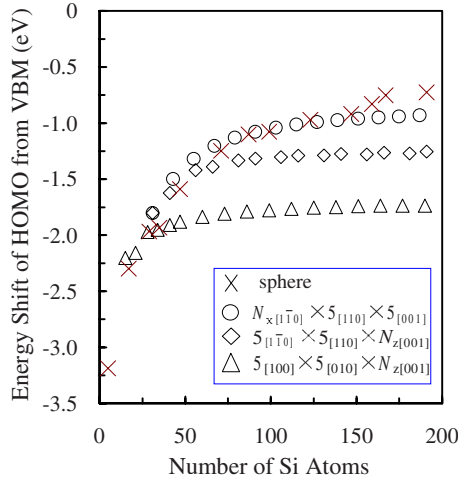


FIG. 4. (Color online) Calculated energy shifts of the HOMO state from the bulk VBM (valence-band maximum) as a function of the number of Si atoms contained in the QBs and quantum spheres studied.

contained. The reason for the latter is as follows: at first, it is noted that H passivation of Si nanocrystals not only eliminates dangling-bond states out of the energy gap between the HOMO and LUMO levels but also forms a surface barrier for confining electrons and holes. A quantum-confinement effect in Si nanocrystals or a blueshift in energy gap should be based on the action of H-Si bonds as a surface barrier. The formation of the surface barrier is ascribed to the bonding-antibonding splitting of the H-Si bonds around the energy gap. The larger the splitting is, the more significant the confinement of carriers is. The H-Si bonding-antibonding splitting can be regarded as tantamount to a vacuum barrier when it is sufficiently large. On the other hand, the peak of the density of Si-H antibonding states produced by the formation of H-Si bonds on the Si surface occurs around 1.2 eV above the conduction-band minimum or 2.3–2.4 eV above the valence-band maximum (VBM) of the infinite Si bulk.<sup>9</sup> Those Si-H antibonding states, which act as a surface barrier for electrons at the LUMO level of a Si nanocrystal, can mix more or less with the LUMO level because of a large upward energy shift in the latter due to quantum confinement. As a result, the function of the H-Si antibonding states as a surface barrier can fall down. The resulting decline of the action of the H-Si antibonding states as a surface barrier for electrons would lead to a pinning of the LUMO energies with respect to the variation in the number of Si atoms contained.

The size dependence of the energy shift of the HOMO level (lowering of the HOMO energy) from the bulk VBM is shown in Fig. 4 for all Si nanocrystals studied. We can see that the HOMO energies are, on the whole, controlled by quantum-confinement effects, and that the HOMO energies of the QBs are well controlled by two-dimensional quantum confinement for the larger number of Si atoms contained. The HOMO level in the  $5_{[100]} \times 5_{[010]} \times N_{z[001]}$  QB exhibits the largest energy shift, reflecting the smallest cross section along the (001) plane. On the other hand, the HOMO energy for the  $5_{[1\bar{1}0]} \times 5_{[110]} \times N_{z[001]}$  QB is lower than that for the  $N_{x[1\bar{1}0]} \times 5_{[110]} \times 5_{[001]}$  QB, which is responsible for the wider

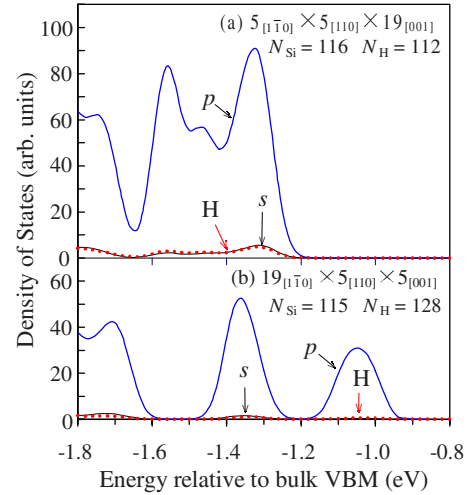


FIG. 5. (Color online) Calculated orbital density of states for Si and H near the HOMO level in the (a)  $5_{[1\bar{1}0]} \times 5_{[110]} \times 19_{[001]}$  and (b)  $19_{[1\bar{1}0]} \times 5_{[110]} \times 5_{[001]}$  QBs. The energy is referred to the VBM of the infinite Si bulk.

energy gap in the former, as mentioned above. The problem here is why this additional shift (lowering) in the HOMO energy happens to the  $5_{[1\bar{1}0]} \times 5_{[110]} \times N_{z[001]}$  QB, despite the fact that its larger cross section suggests a weaker effect of two-dimensional confinement.

The relation in the HOMO energy between the  $5_{[1\bar{1}0]} \times 5_{[110]} \times N_{z[001]}$  and  $N_{x[1\bar{1}0]} \times 5_{[110]} \times 5_{[001]}$  QBs is explained by the orbital character of the HOMO level. Figure 5 shows the ODOS for Si and H near the HOMO level calculated for the (a)  $5_{[1\bar{1}0]} \times 5_{[110]} \times 19_{[001]}$  and (b)  $19_{[1\bar{1}0]} \times 5_{[110]} \times 5_{[001]}$  QBs. Here, the ODOS for Si demonstrates the orbital (*s*- or *p*-like) character of the Si states. These QBs have been selected for the convenience of comparison because they have almost the same number of Si atoms contained ( $N_{Si}=116$  for the  $5_{[1\bar{1}0]} \times 5_{[110]} \times 19_{[001]}$  QB and  $N_{Si}=115$  for the  $19_{[1\bar{1}0]} \times 5_{[110]} \times 5_{[001]}$  QB). As seen in Fig. 5, the HOMO level of the  $5_{[1\bar{1}0]} \times 5_{[110]} \times 19_{[001]}$  QB is composed of *p*-like states with some amount of *s*-like Si and H states while that of the  $19_{[1\bar{1}0]} \times 5_{[110]} \times 5_{[001]}$  QB is somewhat higher in energy and has little amount of *s*-like Si and H states but almost pure *p*-like states of Si. Evidently, it is the H passivation that introduces some amount of H contribution into the HOMO level of the  $5_{[1\bar{1}0]} \times 5_{[110]} \times 19_{[001]}$  QB. The H contribution induces the Si *s* component into the HOMO level, as shown in Fig. 5(a), which would in turn reduce the size of *p-p* interactions in the QB. As is generally known, the *p-p* interactions control the energy around the VBM in the Si bulk (or the HOMO level in Si nanocrystals). More specifically, the stronger the *p-p* interactions are, the higher the energy of the VBM (or the HOMO level) is. Thus, the introduction of the Si *s* component into the HOMO level through the H passivation reduces the size of *p-p* interactions, downshifting the HOMO energy (widening the energy gap) in the  $5_{[1\bar{1}0]} \times 5_{[110]} \times 19_{[001]}$  QB, as shown in Fig. 5(a).

After all, H passivation of a Si nanocrystal would make a core-Si atom (not bonded to H) as well as a Si atom bonded to H distinctly different from bulk Si. In other words, H

orbitals permeate into Si and correlate significantly with Si states through interactions between hydride units and Si atoms. The correlation could not be limited in the surface region where Si atoms are bonded to H atoms, going deeply into core-Si atoms. As mentioned above, this correlation results in inducing the  $s$  component into the HOMO level and reducing the size of Si  $p$ - $p$  interactions, downshifting the HOMO energy. This effect should be more pronounced in smaller Si nanocrystals, where the number of Si atoms bonded to H is much larger than that of core-Si atoms. Thus, H passivation not only eliminates dangling-bond states out of the energy gap but also significantly influences the character of the HOMO state and thereby contributes to the widening of the energy gap. We tentatively refer to the above-mentioned effect of H passivation on the electronic structure as a quasialloying effect in this paper because this effect would be analogous to an alloying effect observed in a binary alloy,<sup>16</sup> by which the character of a binary alloy AB is made different from that of the component A and/or that of the component B.

As stated above, we can expect the quasialloying effect to be more pronounced, when the ratio of the number of Si atoms bonded to H to that of the core-Si atoms contained is higher. Actually, the number of H atoms bonded to the  $19_{[1\bar{1}0]} \times 5_{[110]} \times 5_{[001]}$  QB ( $N_H=128$ ) is somewhat larger than that bonded to the  $5_{[1\bar{1}0]} \times 5_{[110]} \times 19_{[001]}$  QB ( $N_H=112$ ), as shown in Fig. 5. As is well known, however, when terminated by hydrogen, the (110) planes of Si form monohydrides (Si-H bonds) while the (100) planes form dihydrides (Si-H<sub>2</sub> bonds). Therefore, a considerable amount of H atoms bonded to the  $19_{[1\bar{1}0]} \times 5_{[110]} \times 5_{[001]}$  QB form dihydrides on the two elongated (001) surfaces of the QB, resulting in a larger number of remaining core-Si atoms contained. This in turn indicates a weaker quasialloying effect on the HOMO level. In fact, the H passivation gives little amount of H contribution to the HOMO level of the  $19_{[1\bar{1}0]} \times 5_{[110]} \times 5_{[001]}$  QB, as shown in Fig. 5(b). As a result, the HOMO energy of the  $19_{[1\bar{1}0]} \times 5_{[110]} \times 5_{[001]}$  QB would be determined mainly by a quantum-confinement effect. On the other hand, the HOMO energy of the  $5_{[1\bar{1}0]} \times 5_{[110]} \times 19_{[001]}$  QB is downshifted by a quasialloying effect in addition to a quantum-confinement effect. In this sense, we can say that a quasialloying effect on the HOMO level is sensitive to the shape of the QBs.

We can compare the calculated energy shift in the HOMO level with an experimental observation in porous Si, because, as is well known, Si nanocrystals in as-prepared porous Si are passivated with hydrogen.<sup>1</sup> Energy shifts in the HOMO and LUMO levels have been measured by photoemission and x-ray absorption spectroscopy in porous Si, which has clarified that the HOMO shift from the bulk is about twice as large as the LUMO shift.<sup>17</sup> However, the recent semiempirical tight-binding calculations for Si nanocrystals and nanowires passivated with hydrogen, which have discussed the size dependence of energy gaps on the basis of the quantum-confinement model, have shown that calculated energy shifts of the HOMO level (valence-band edge) from the bulk are smaller than those of the LUMO level (conduction-band edge) at a small radius of the nanocrystal or nanowire,<sup>8</sup> in disagreement with the measurement in porous Si.<sup>17</sup> It is

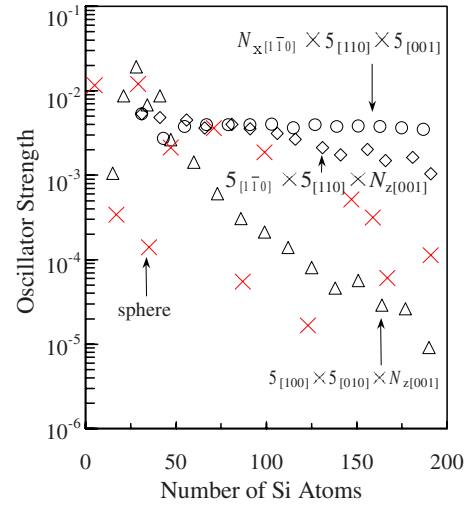


FIG. 6. (Color online) Calculated oscillator strengths across the energy gap as a function of the number of Si atoms contained in the QBs and quantum spheres studied.

likely that this discrepancy has been caused by strengthening the H-Si bonds (by assuming very large interactions between H and Si atoms) for removing dangling-bond states out of the energy gap.<sup>18</sup> Strengthening of the H-Si bonds leads to a very large H-Si bonding-antibonding splitting and thus their function as a surface barrier is enhanced, and then, carriers at the HOMO and LUMO levels are well confined.<sup>16</sup> Thus, it would be obvious that the larger HOMO shift observed in porous Si (Ref. 17) cannot be explained solely by the quantum-confinement model. On the other hand, the additional energy shift due to a quasialloying effect on the HOMO level, as stated above, could qualitatively explain the larger HOMO shift observed in porous Si.

## B. Oscillator strength and lifetime

Figure 6 shows the calculated oscillator strength for optical transitions across the energy gap between the HOMO and LUMO states in the Si QBs and quantum spheres studied as a function of the number of Si atoms contained. We see an overall trend expected from the quantum-confinement model in which the oscillator strength should decrease monotonically with an increase in the number of Si atoms (or the QB size). We find that the oscillator strength calculated for the  $N_x[1\bar{1}0] \times 5_{[110]} \times 5_{[001]}$  QB is somewhat larger than that for the  $5_{[1\bar{1}0]} \times 5_{[110]} \times N_z[001]$  QB. Obviously, the oscillator strengths for both QBs are mainly controlled by two-dimensional quantum confinement and slowly decrease with the increase in the number of Si atoms. On the other hand, the oscillator strength calculated for the  $5_{[100]} \times 5_{[010]} \times N_z[001]$  QB does not seem to be controlled by two-dimensional quantum confinement along the [100] and [010] directions but sharply decreases with the increase in the number of Si atoms along the [001] direction. The reason for this trend is as follows: the calculations show that while the LUMO states in both the  $N_x[1\bar{1}0] \times 5_{[110]} \times 5_{[001]}$  and  $5_{[1\bar{1}0]} \times 5_{[110]} \times N_z[001]$  QBs are mostly bulklike (delocalized), the LUMO state in the  $5_{[100]} \times 5_{[010]} \times N_z[001]$  QB is somewhat

lower in energy and has a more surfacelike nature. In other words, effects of penetration of a LUMO wave function outside the  $5_{[100]} \times 5_{[010]} \times N_{z[001]}$  QB are significant. This surfacelike nature of the LUMO state arises from the heavy mixing of the LUMO level with the Si-H antibonding states (due to interhydride interactions<sup>13</sup>), as stated above. Thus, the LUMO level in the  $5_{[100]} \times 5_{[010]} \times N_{z[001]}$  QB is associated closely with hydrogen on the surface. As a result, electrons at the H-related LUMO state in this QB are not well confined in the QB but localized on the surface, failing to contribute to the oscillator strength.

We observe a large scatter in the oscillator strength calculated for the quantum spheres in Fig. 6. The reason for this is as follows: the oscillator strength or transition probability is generally sensitive to the symmetry of both HOMO and LUMO states, which in turn depends on the geometry of the nanocrystals including the granularity of the surface. Most of Si atoms in an ultrasmall sphere are on or near the surface and would be largely affected by possible surface effects. Also, interatomic interactions between H atoms through the underlying Si atoms can be reflected in the wild variance in the oscillator strength. Furthermore, three-dimensional quantum confinement expected for the quantum spheres under such an ultrasmall size regime as in the range of Si atoms up to as many as 200 can significantly alter the lowest conduction-band states of Si and thus make the electronic structure of the LUMO level very intricate. Thus, we can say that the large scatter in the oscillator strength reflects sensitivity to the detailed structure of the surface as well as the symmetry of the quantum spheres.

Figure 7 shows the calculated radiative lifetimes as a function of photon energy (energy gap), for the convenience of comparison with experiment. It is found that the transitions are mostly dipole allowed and the lifetimes are less than  $\sim 100 \mu\text{s}$ , which are of the same order of magnitude as those measured in PL from light-emitting porous Si and Si nanocrystals embedded in  $\text{SiO}_2$ .<sup>19–22</sup>

Judging from the fact that the Si  $5_{[1\bar{1}0]} \times 5_{[110]} \times N_{z[001]}$  and  $N_{x[1\bar{1}0]} \times 5_{[110]} \times 5_{[001]}$  QBs studied here present the energy gaps around 3.3 eV (in a blue light regime) with the lifetime of less than  $1 \mu\text{s}$ , we can say that these QBs studied have some potential to emit blue light.

Finally, it is noted that the sensitivity of the electronic structure of the QBs studied here to the choice of the EHNTB parameters used (including relaxation of the atomic coordinates or bond lengths) has been tested, and the characteristic features of the HOMO and LUMO levels are not so sensitive to the choice of the EHNTB parameters used, at

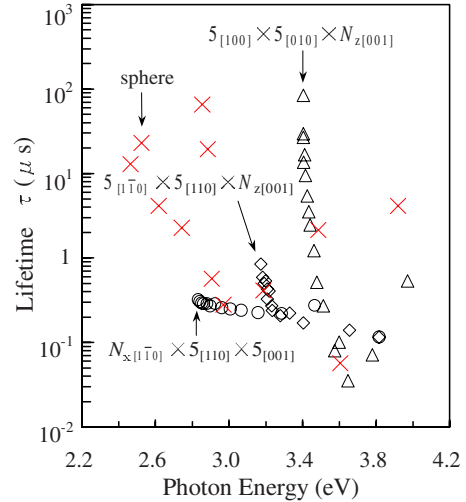


FIG. 7. (Color online) Calculated lifetimes ( $\mu\text{s}$ ) as a function of photon energy (energy gap, electron volt) for the QBs and quantum spheres studied.

least qualitatively, but persist for a reasonable range of the parameters.

#### IV. CONCLUSIONS

The electronic structure of the Si  $5_{[1\bar{1}0]} \times 5_{[110]} \times N_{z[001]}$ ,  $N_{x[1\bar{1}0]} \times 5_{[110]} \times 5_{[001]}$ , and  $5_{[100]} \times 5_{[010]} \times N_{z[001]}$  QBs passivated with hydrogen has been calculated by the EHNTB method and compared with that of the quantum spheres. It has been emphasized that the electronic structure of the Si QBs passivated with hydrogen cannot be explained by the widely used quantum-confinement model alone.

Although the  $5_{[1\bar{1}0]} \times 5_{[110]} \times N_{z[001]}$  QB suggests an effect of weaker (two-dimensional) quantum confinement than the  $N_{x[1\bar{1}0]} \times 5_{[110]} \times 5_{[001]}$  QB, the former exhibits a larger energy gap than the latter. This has been explained by a quasilloying effect on the HOMO level, which has been found to be sensitive to the shape of the QBs. The oscillator strength calculated for the  $N_{x[1\bar{1}0]} \times 5_{[110]} \times 5_{[001]}$  QB is larger than that for the  $5_{[1\bar{1}0]} \times 5_{[110]} \times N_{z[001]}$  QB, as expected from the quantum-confinement model. In contrast, the oscillator strength calculated for the  $5_{[100]} \times 5_{[010]} \times N_{z[001]}$  QB is not well controlled by two-dimensional quantum confinement along the  $[100]$  and  $[010]$  directions but decreases sharply with an increase in the number of Si atoms. The latter has been explained by the occurrence of a H-related surface state at the LUMO level, which is also sensitive to the shape of the QBs.

<sup>1</sup>A. G. Cullis, L. T. Canham, and P. D. J. Calcott, *J. Appl. Phys.* **82**, 909 (1997); O. Bisi, S. Ossicini, and L. Pavesi, *Surf. Sci. Rep.* **38**, 1 (2000).

<sup>2</sup>W. L. Wilson, P. F. Szajowski, and L. E. Brus, *Science* **262**, 1242 (1993).

<sup>3</sup>W. Lu and C. M. Lieber, *J. Phys. D* **39**, R387 (2006).

<sup>4</sup>T. P. Pearsall, J. Bevk, L. C. Feldman, J. M. Bonar, J. P. Mannaerts, and A. Ourmazd, *Phys. Rev. Lett.* **58**, 729 (1987).

<sup>5</sup>R. Tsu, *Nature (London)* **364**, 19 (1993); D. J. Lockwood, Z. H. Lu, and J.-M. Baribeau, *Phys. Rev. Lett.* **76**, 539 (1996).

<sup>6</sup>M. Nishida, *Phys. Rev. B* **75**, 235306 (2007).

<sup>7</sup>F. Trani, G. Cantele, D. Ninno, and G. Iadonisi, *Phys. Rev. B* **72**,

- 075423 (2005).
- <sup>8</sup>Y. M. Niquet, C. Delerue, G. Allan, and M. Lannoo, *Phys. Rev. B* **62**, 5109 (2000); Y. M. Niquet, A. Lherbier, N. H. Quang, M. V. Fernández-Serra, X. Blase, and C. Delerue, *ibid.* **73**, 165319 (2006).
- <sup>9</sup>M. Nishida, *Phys. Rev. B* **58**, 7103 (1998); **59**, 15789 (1999); **60**, 8902 (1999).
- <sup>10</sup>Y. Dai, S. Han, D. Dai, Y. Zhang, and Y. Qi, *Solid State Commun.* **126**, 103 (2003).
- <sup>11</sup>E. Degoli, G. Cantele, E. Luppi, R. Magri, D. Ninno, O. Bisi, and S. Ossicini, *Phys. Rev. B* **69**, 155411 (2004).
- <sup>12</sup>M. Lopez del Puerto, M. Jain, and J. R. Chelikowsky, *Phys. Rev. B* **81**, 035309 (2010).
- <sup>13</sup>M. Nishida, *Solid State Commun.* **121**, 127 (2002); *Phys. Rev. B* **66**, 125313 (2002).
- <sup>14</sup>P. K. Basu, *Theory of Optical Processes in Semiconductors* (Oxford University Press, New York, 1997), p. 43.
- <sup>15</sup>W. B. Jackson and N. M. Johnson, in *Microscopic Identification of Electronic Defects in Semiconductors*, MRS Symposia Proceedings No. 46, edited by N. M. Johnson, S. G. Bishop, and G. Watkins (Materials Research Society, Pittsburgh, 1985), p. 545.
- <sup>16</sup>M. Nishida, *Phys. Rev. B* **70**, 113303 (2004).
- <sup>17</sup>T. van Buuren, T. Tiedje, J. R. Dahn, and B. M. Way, *Appl. Phys. Lett.* **63**, 2911 (1993).
- <sup>18</sup>J. P. Proot, C. Delerue, and G. Allan, *Appl. Phys. Lett.* **61**, 1948 (1992); C. Delerue, G. Allan, and M. Lannoo, *Phys. Rev. B* **48**, 11024 (1993).
- <sup>19</sup>G. W. 't Hooft, Y. A. R. R. Kessener, G. L. J. A. Rikken, and A. H. J. Venhuizen, *Appl. Phys. Lett.* **61**, 2344 (1992).
- <sup>20</sup>I. Mihalcescu, J. C. Vial, and R. Romestain, *Phys. Rev. Lett.* **80**, 3392 (1998).
- <sup>21</sup>M. V. Wolkin, J. Jorne, P. M. Fauchet, G. Allan, and C. Delerue, *Phys. Rev. Lett.* **82**, 197 (1999).
- <sup>22</sup>C. Garcia, B. Garrido, P. Pellegrino, R. Ferre, J. A. Moreno, and J. R. Morante, *Appl. Phys. Lett.* **82**, 1595 (2003).